J IRAN CHEM SOC (2012) 9:671–680
DOI 10.1007/s13738-012-0150-z

ORIGINAL PAPER

Synthesis, characterization and DNA-binding characteristics of Ru(II) molecular light switch complexes

C. Shobha Devi · Penumaka Nagababu · M. Shilpa · Y. Praveen Kumar · M. Rajender Reddy · Nazar Md Gabra · S. Satyanarayana

Received: 8 October 2011 / Accepted: 14 January 2012 / Published online: 22 August 2012

Abstract A series of four polypyridyl Ru(II) complexes such as $[Ru(L)_4(PIP)]^{2+}$ and $[Ru(L)_4PPIP]^{2+}$ where L is 4-amino pyridine and Pyridine (PIP = 2-phenylimidazo[4,5-f] [1, 10] phenanthroline), (PPIP = 2-(4′-phenoxy-phenyl) imidazo[4,5-][1, 10]phenanthroline) have been synthesized and characterized by elemental analysis, physicochemical methods such as UV–vis, IR and NMR spectroscopic techniques. The DNA-binding behavior of these complexes was investigated by electronic absorption titrations, fluorescence spectroscopy, viscosity measurements and salt-dependent studies. The experimental results indicate that all these complexes can bind to DNA through an intercalation mode, the DNA-binding affinities of these complexes follow the order $[Ru(4\text{-}APy)_4(PPIP)]^{2+}$(**1**) > $[Ru(Py)_4PPIP]^{2+}$(**2**) > $[Ru(4\text{-}APy)_4(PIP)]^{2+}$(**3**) > $[Ru(Py)_4PIP]^{2+}$(**4**). Noticeably, these complexes have been found to be efficient photosensitisers for strand scissions in plasmid DNA. Further, all four complexes screened for their antimicrobial activity indicate that the complexes show appreciable activity against *Escherichia coli* and *Neurospora Crassa*. In addition, in the presence of Co^{2+}, the emission of DNA-$[Ru(L_4)PPIP/PIP]^{2+}$ can be quenched and recovered by the addition of EDTA, which exhibited the DNA "light switch" properties.

Keywords Ru(II)complexes · Calf-thymus DNA · Emission quenching · Light switch effect · Photocleavage

C. Shobha Devi · M. Shilpa · Y. Praveen Kumar · M. Rajender Reddy · N. M. Gabra · S. Satyanarayana (✉)
Department of Chemistry, Osmania University, Hyderabad 500 007, Andhra Pradesh, India
e-mail: ssnsirasani@gmail.com

P. Nagababu
Institute of Chemistry, Academia Sinica, Taipei, Taiwan

Abbreviations

PIP	[2-Phenylimidazo [4,5-f] [1, 10] phenanthroline]
PPIP	[2-(4′-Phenoxy-phenyl) imidazo[4,5-f][1, 10] phenanthroline]
Py	Pyridine
4-APy	4-Aminopyridine
Bpy	2,2′-Bipyridine
Phen	1,10-Phenanthroline
Dmb	4,4′-Dimethyl-2,2′-bipyridine
Dip	4,4′-Diphenyl-2,2′-bipyridine
EB	Ethidium bromide
DMSO	Dimethylsulphoxide
TMS	Tetramethylsilane
EDTA	Ethylenediaminetetraacetic acid
CT DNA	Calf thymus DNA

Introduction

There has been great deal of interest on Ru(II) polypyridyl complexes owing to their wide range of applications in various fields such as photophysics [1], photochemistry, supramolecular chemistry [2] and biochemistry [3, 4]. They also play a crucial role in biological processes such as respiration, photosynthesis and oxidative DNA cleavage [5]. From the literature study, it is evident that many Ru(II) polypyridyl complexes with their planar aromatic ligands can intercalate through DNA base pairs. These small molecules binding to DNA are very important in the development of new chemotherapeutic reagents [6–9], base pair mismatches and DNA molecular probes. Because of their feasibility in the synthesis, strong luminescent

characteristics and DNA-binding affinity, Ru(II) intercalators became targets for many researchers [10, 11].

DNA may have potential application as a template or as an element in DNA-based nanocircuits and molecular electronics including photo electronics. A requirement for the latter is a means to switch the photoactive molecule on and off; otherwise, irradiation always results in charge transport. This requirement can be fulfilled by Ru(II) polypyridyl complexes, since these complexes can also function as "molecular light switches" in aqueous solution, exhibiting weak luminescence in the absence of DNA and strong luminescence upon addition of DNA. Most of the studies of DNA binding with metal complexes have emphasized on intercalative than auxiliary ligands. However, Ji et al. [12–15] have studied role of auxiliary ligands in polypyridyl Ru(II) complexes for their interaction with DNA. The auxiliary ligand of polypyridyl ruthenium(II) complexes plays a key role in the spectral properties and interaction with DNA [16]. But the intercalating ligand in the complex is the polypyridyl ligand not the ancillary ligand.

In most of the compounds described so far, the Ru(II) metal center is bound to bidentate aromatic and polyaromatic compounds such as bpy, phen, dmb and dip [17, 18]. Less attention has been paid to compounds containing monodentate ligands. Particularly, Ru(II)-PIP/PPIP complexes with four pyridines/aminopyridines have not been reported yet. In this contribution, we report synthesis and characterization of four ruthenium polypyridyl complexes $[Ru(4\text{-}APy)_4(PPIP)]^{2+}$, $[Ru(Py)_4PPIP]^{2+}$, $[Ru(4\text{-}APy)_4(PIP)]^{2+}$ and $[Ru(Py)_4PIP]^{2+}$. Their interactions with DNA were investigated by electronic absorption, emission quenching studies, viscosity and salt-dependent studies. Effects of light switching on and off were also studied. These complexes can intercalate into DNA base pairs and cleave the pBR 322 DNA with high activity upon irradiation. We have also tested all four complexes for their antimicrobial activity.

Experimental

Materials

All reagents and solvents were purchased commercially and were used as received unless otherwise noted. $RuCl_3$, 1,10-Phenanthroline monohydrate and pyridines were purchased from Merck, calf thymus (CT) DNA was purchased from Aldrich and supercoiled pBR 322 DNA was obtained from Fermentas life sciences. Double distilled water was used for preparing various buffers. Interaction of the complexes with DNA was studied in tris buffer (5 mM Tris HCl, 50 mM NaCl, pH 7.2). The DNA had a ratio of UV absorbance at 260 and 280 nm of about 1.8–1.9:1, indicating that the DNA was sufficiently free of protein [19]. The concentration of DNA per nucleotide was determined by spectroscopy using a molar absorption coefficient of 6,600 M^{-1} cm^{-1} (260 nm) [20].

Synthesis and characterization

1,10-Phenanthroline-5,6-dione [21], PIP[PIP = 2-phenylimidazo[4,5-f] [1, 10] phenanthroline], PPIP[PPIP = 2-(4′-phenoxy-phenyl) imidazo[4,5-][1, 10]phenanthroline] [22] and $[Ru(L)_4Cl_2]^{2+}$ [23] were synthesized according to the literature procedure. Synthetic strategies of these ligands and their Ru(II) complexes are shown in Fig. 1.

Synthesis of compound 1

Tetra 4-aminopyridine, 2-(4′-phenoxy-phenyl) imidazo[4,5-f][1, 10]phenanthroline ruthenium(II) perclorate was synthesized by mixing $[Ru(4\text{-}APy)_4Cl_2]\cdot 2H_2O$ (0.5 mM) and PPIP (0.5 mM) in 25 mL ethanol and 15 mL water. This mixture was refluxed for 8 h under nitrogen atmosphere to give a clear and red solution. After cooling, the solution was treated with a saturated aqueous solution of sodium perchlorate to give red precipitate. The red solid was collected and washed with 2 mL of ice cooled ethanol, then it was dried in vacuo. Yield: 70 %. Anal. calcd. for (%) $C_{45}H_{44}N_{12}O_{11}Cl_2Ru$ C, 49.1; H, 4.03; N, 15.27. Found (%): C, 49.15; H, 4.1; N, 15.5. IR (KBr) 3,445 (broad) (N–H), 1,654 (C=N), 1,540 (C=C), 550 cm^{-1} (Ru–N). ^{1}H-NMR (DMSO-d_6, 400 MHz): δ9.1 (m, 2H, H_1, H_3), δ8.3 (m, 2H, H_{16}, H_{17}), δ8.1 (d, 1H, H_2), δ7.8 (m, 2H, H_8, H_9), δ7.5 (t, 1H, H_{14}), δ7.3 (t, 1H, H_{13}), δ7.1 (t, 1H, H_{12}), δ3.5 (NH_2), δ2.1 (NH).

Synthesis of compound 2

Tetra 4-pyridine, 2-(4′-phenoxy-phenyl) imidazo[4,5-f][1, 10] phenanthroline ruthenium(II) perchlorate was obtained by a similar procedure to that described above, $[Ru(Py)_4Cl_2]\cdot 2H_2O$ (0.5 mM) was used in place of $[Ru(4\text{-}APy)_4Cl_2]\cdot 2H_2O$. Yield: 65 %. Anal. calcd. for (%) $C_{45}H_{40}N_8O_{11}Cl_2Ru$ C, 51.93; H, 3.87; N, 10.77. Found (%): C, 52.2; H, 3.92; N, 11.05. IR (KBr) 3,447 (N–H), 1,652 (C=N), 1,560 (C=C), 549 cm^{-1} (Ru–N). ^{1}H-NMR (DMSO-d_6, 400 MHz): δ9.4 (d, 1H, H_1), δ8.6 (d, 1H, H_{16}), δ8.5 (t, 1H, H_2), δ8.45 (d, 1H, H_3), δ8.4 (t, 1H, H_{18}), δ8.3 (t, 1H, H_{17}), δ8.22 (d, 1H, H_8), δ8.2 (m, 2H, $H_{9,12}$), δ8.0 (d, 1H, H_{13}), δ7.8 (d, 1H, H_{14}), δ2.2 (NH). ^{13}C[^{1}H]-NMR (DMSO-d_6, 400 MHz): δ157.8 (1C, C_1), δ156.7 (1C, C_{15}), δ154.2 (1C, C_5), δ150.0 (1C, C_{16}), δ136.9 (1C, C_4), δ136.0 (1C, C_6), δ130.5 (1C, C_3), δ129.0 (1C, C_{17}), δ128.0 (1C, C_{18}), δ125.0

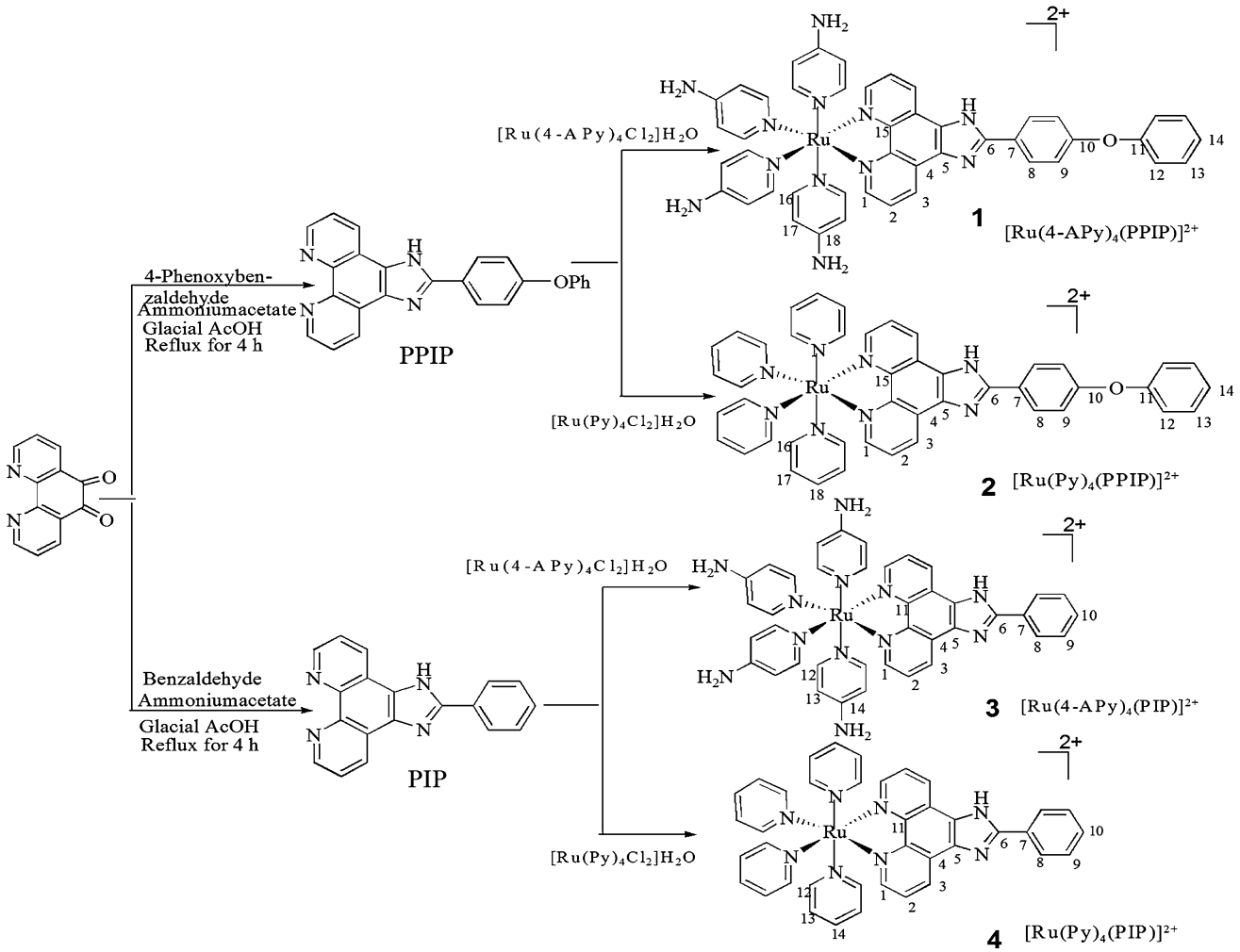

Fig. 1 Synthetic routs for ligand and 1, 2, 3 and 4 complexes

(1C, C_2), δ124.6 (2C, $C_{8,9}$), δ124.0 (1C, C_{10}), δ123.0 (2C, $C_{7,14}$), δ120.4 (1C, C_{11}), δ119.7 (1C, C_{13}), δ119.0 (1C, C_{12}).

Synthesis of compound 3

Tetra 4-aminopyridine, 2-phenylimidazo[4,5-f] [1, 10] phenanthroline ruthenium(II) perchlorate complex was obtained by a similar procedure to that described above; PIP (0.5 mM) was used in place of PPIP. Yield: 75 %. Anal. calcd. for (%) $C_{39}H_{41}N_{12}O_{10}Cl_2Ru$ C, 46.42; H, 4.06; N, 16.66. Found (%): C, 46.56; H, 4.1; N, 16.78. IR (KBr) 3,373 (broad) (N–H), 1,636 (C=N), 1,516 (C=C), 550 cm^{-1} (Ru–N) ^{1}H-NMR (DMSO-d_6, 400 MHz): δ9.1 (d, 1H, H_{12}), δ8.10 (m, 2H, $H_{1,}$ H_{13}), δ7.9 (m, 2H, H_2, H_9), δ7.7 (d, 1H, H_3), δ7.6 (d, 1H, H_{10}), δ7.5 (d, 1H, H_8), δ3.10(NH_2), δ2.1 (NH). ^{13}C [^{1}H]-NMR (DMSO-d_6, 400 MHz): δ156.1 (1C, C_1), δ144.7 (2C, $C_{11,12}$), δ129 (1C, C_2), δ128.8 (1C, C_3), δ126.9 (1C, C_4), δ110.9 (2C, $C_{5,14}$), δ109.5 (1C, C_{13}), δ108.9 (2C, $C_{6,7}$), δ108.0 (1C, C_{10}), δ107.0(2C, $C_{9,8}$).

Synthesis of compound 4

Tetra pyridine, 2-phenylimidazo[4,5-f] [1, 10] phenanthroline] ruthenium(II) perchlorate complex was obtained by a similar procedure to that described above, $[Ru(Py)_4Cl_2]\cdot 2H_2O$ (0.5 mM) was used in place of $[Ru(4\text{-}APy)_4Cl_2]\cdot 2H_2O$. Yield: 75 %. Anal. calcd. for (%) $C_{39}H_{36}N_8O_{10}Cl_2Ru$ C, 49.36; H, 3.9; N, 11.84. Found (%): C, 49.38; H, 4.051; N, 11.479. IR (KBr) 3,368 (broad) (N–H), 1,650 (C=N), 1,560 (C=C), 549 cm^{-1} (Ru–N) ^{1}H-NMR (DMSO-d_6, 400 MHz): δ8.4 (m, 2H, $H_{1,}$ H_{11}), δ8.0 (m, 3H, $H_{2,}$ $H_{7,}$ H_{12}), δ7.6 (m, 2H, $H_{9,}$ H_{13}), δ6.7 (d, 1H, H_3), δ6.6 (d, 1H, H_8), δ2.5 (NH).

Physical measurements

UV–visible spectra were recorded with an Elico SL159 spectrophotometer. IR spectra were recorded on KBr disks on a Perkin-Elmer FT-IR-1605 spectrometer. ^{1}H and ^{13}C NMR spectra were recorded on a Bruker 400 MHz spectrometer with DMSO as solvent at RT and TMS as the internal standard. Microanalyses (C, H, N) were carried out with a Perkin-Elmer 240 elemental analyzer. Absorption titration experiment was performed at room temperature to determine the binding affinity between the DNA and complex. A fixed ruthenium concentration 3.0 ml (20 μM) was taken in a cuvette to which increments of the DNA stock solution were added. DNA solution (concentration 30–200 μM per nucleotide) was added to each cuvette reference and sample to eliminate the absorbance of DNA itself. Solutions were mixed for 3 min and absorption spectra were recorded. Titrations were continued until there was no further change in the spectra was noted. Fluorescence measurements were performed on a Hitachi F-2500 spectrofluorimeter. All measurements were made at 25 °C using a thermostated cuvette holder. Emission titration experiments were performed at a fixed metal complex concentration (10 μM) to which increments of a DNA solution (10–150 μM) were added. Viscosity experiments were carried out on Ostwald viscometer immersed in thermostated water bath maintained at 30 ± 0.1 °C. Flow time was measured with a digital stopwatch and every sample was measured three times and an average flow time was calculated. Data were presented as $(\eta/\eta_o)^{1/3}$ versus the concentration of [Ru(II)]/[DNA] [36], where η is the viscosity of DNA in the presence of complexes and η_o is the viscosity of DNA alone. For gel electrophoresis experiments, supercoiled pBR 322 DNA(0.1 μg/μL) was treated with 20–80 μM of Ru(II) complexes and the mixtures were irradiated at 365 nm for 1 h. The samples were then analyzed by 0.8 % agarose gel electrophoresis (Tris–Acetic acid-EDTA buffer, pH 8.0) at 50 V for 2 h. The gel was stained with 1 μg ethidium bromide and photographed under UV light. The antibacterial activity of the complexes was studied against *Escherichia coli* and *Neurospora crassa*. Each of the Ru(II) complex was dissolved in DMSO at a concentration of 1 mg mL^{-1}. Paper disks of Whatman filter paper no. 1 were sterilized in an autoclave. The paper disks saturated with 10 μL of the Ru(II) complex were placed in the Petri dishes containing LB (Luria Bertini) agar media inoculated with *E. coli* and *N. crassa* separately. The Petri dishes were incubated at 37 °C and the inhibition zones were recorded after 24 h of incubation. The results were also compared with standard antibacterial drug Ampicillin at the same concentration.

Results and discussion

Electronic absorption titration

The application of electronic absorption spectroscopy in DNA-binding studies of Ru-polypyridyl complexes is one of the most useful techniques [24–26]. A complex binding to DNA through intercalation usually results in hypochromism and bathochromism, due to the intercalation mode involving a strong π–π^* stacking interaction between an aromatic chromophore and the base pairs of DNA [22]. It is generally accepted that the extent of the hypochromism in the UV–visible band is consistent with the strength of intercalative interaction [27–30]. The absorption spectra of complexes **1–4** in the absence and presence of CT-DNA (at constant concentration of complex, i.e., 10–15 μM) are given in Fig. 2. As the concentration of DNA increases, absorption bands of the complexes display clear hypochromism. An insignificant red shift in the MLCT band of the complexes was observed. The hypochromism ($H\ \% = 100x\ (A_{free} - A_{bound})/A_{free}$) of the MLCT bands at 469, 466, 471 and 475 of complexes **1–4** was determined to be about 11.5, 9.41, 16.2 and 12.4 %, respectively. To compare the DNA-binding affinities of all four complexes, quantitatively, their intrinsic binding constant K_b to DNA was obtained by monitoring the changes of the MLCT absorbance at their respective wavelengths, according to the following Eq. [31].

$$[DNA]/(\varepsilon_a - \varepsilon_f) = [DNA]/(\varepsilon_b - \varepsilon_f) + 1/K_b(\varepsilon_b - \varepsilon_f)$$

where [DNA] is the concentration of DNA in nucleotides, ε_a,ε_f and ε_b are the extinction coefficient for the free Ru(II) complex, extinction coefficient of complex in the presence of DNA, and the extinction coefficient of the Ru(II) complex in the fully bound form, respectively. Intrinsic binding constant K_b of complexes is given in Table 1. The K_b values of complexes are in the order of **1** > **2** > **3** > **4**. This suggests that there is a mode of binding that involves a striking interaction between the complex and the base pairs of DNA. As PPIP possesses a greater planar area and extended π system, it penetrates more deeply into the DNA base pairs. Therefore, binding constants for **1**, **2** complexes are more than that of **3** and **4**. The difference in binding strengths of complexes **1** and **2**; **3** and **4** is probably caused by the difference in auxiliary ligands. The four additional NH_2 groups in complexes 1 and 3 may exert some additional interactions (may be H-bonding) with DNA base pairs and hence have higher binding constants. The K_b values are more than those reported earlier for their bidentate ligands $[Ru(bpy)_2PPIP]$ (4.3×10^4) [22]. This difference is due to the difference in the ancillary ligands. When these complexes are bound to DNA, there is no conformational change observed except a change in the

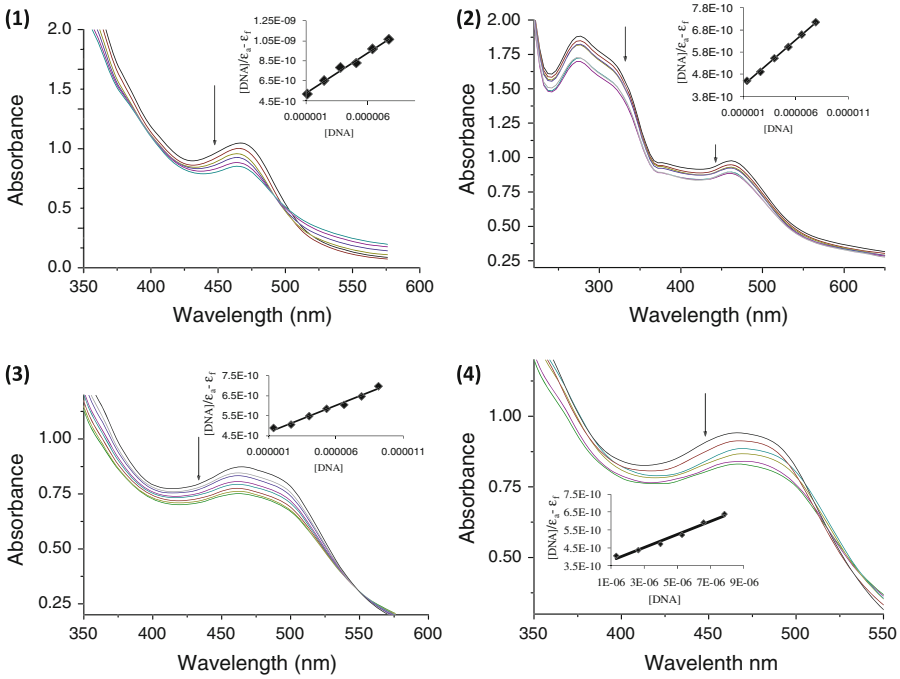

Fig. 2 Absorption spectra of $[Ru(4\text{-}APy)_4(PPIP)]$ (1), $[Ru(Py)_4PPIP]$ (2), $[Ru(4\text{-}APy)_4(PIP)]$ (3) and $[Ru(Py)_4PIP]$(4) in Tris–HCl buffer upon addition of CT-DNA in absence (*top*) and presence of CT-DNA (*lower*) the [complex] = 10–15 μM. [DNA] = 0–120 μM. *Inset* plots of $[DNA]/(\varepsilon_a - \varepsilon_f)$ versus [DNA] for the titration of DNA with Ru(II) complexes. *Arrow* shows change in absorption with increasing DNA concentration

absorption intensity. The DNA is still in B form without conformational change.

Emission studies

All four complexes show emission in Tris buffer at ambient temperature [32]. The excitation peaks appeared at 467, 462, 470 and 464 nm and emission peaks at 588, 598, 591 and 599 nm for **1**, **2**, **3** and **4** complexes, respectively. Upon addition of CT-DNA, the emission intensities increase further than the complex alone as shown in Fig. 3. This implies that complexes can strongly interact with DNA. Binding data were cast into the scatchard plot of r/C_f versus r, where r is the binding ratio (C_b/[DNA]) and C_f is the free ligand concentration. Non linear least square fitting of the data yield K and n, the n exclusion parameter is 3.2(±0.3) bp. The binding constants calculated are also comparable with UV absorption data. The K (emission binding constant) values are given in Table 1.

Emission quenching experiments using $[Fe(CN)_6]^{4-}$ as quencher further support the above proposal. As illustrated in Fig. 4 in the absence of DNA, complexes were efficiently quenched by $[Fe(CN)_6]^{4-}$ resulting in two linear Stern–Volmer plots. In the presence of DNA, quenching was small, because of the highly negatively charged $[Fe(CN)_6]^{4-}$ would be repelled by the negative charge of the DNA phosphate backbone which would hinder the quenching of the emission of the bound complexes. The Stern–Volmer quenching constant K_{sv} can be determined using Stern–Volmer equation [33].

$$I_0/I = 1 + K_{sv}[Q]$$

where I_0 and I are the fluorescence intensities in the absence and presence of quencher, respectively, Q is the concentration of the quencher, K_{sv} is a linear Stern–Volmer quenching constant. In the quenching plot of I_0/I versus [Q], K_{sv} is given by the slope. Figure 4 shows the ferrocyanide quenching plots for complexes in the absence, presence and excess of DNA. All four complexes show linear Stern–Volmer plots. The K_{sv} values for all four complexes are given in Table 1. The quenching studies indicate that the DNA-binding abilities of the complexes follow the order: **1** > **2** > **3** > **4**. These Stern–Volmer plots are linear and complex is cation and quencher is anion, a type of fluorophore–quencher complex (F–Q) is formed. It could be static quenching.

Light switch on off effect

From Fig. 6, it can be seen that after binding to DNA (switch on), the emission of DNA-$[Ru(APy)_4(PPIP)]$ can be quenched by Co^{2+} ion, thus turning the light switch off [34, 35]. The addition of 0.03 mM Co^{2+} to 0.01 mM of complex bound to 0.2 mM DNA results in the loss of luminescence due to the formation of Co^{2+}-$[Ru(APy)_4(PPIP)]$ (heterometallic complex). In order to further provide additional evidence for the quenching which originated in the formation of heterometallic complex, the emission spectra of $[Ru(APy)_4(PPIP)]$ without DNA in the absence and presence of Co^{2+} are measured. Similar quenching of luminescence was observed. This observation

Table 1 Absorption peaks, absorption, emission and quenching binding constants of Ru(II)complexes

Complex	Absorption λ_{max} (nm)	Absorption binding constant K_b (M^{-1})	(K) Emission binding constant	(K_{sv} Only Comp + DNA Comp 1:50 1:200
$[Ru(4\text{-}APy)_4(PPIP)]$	469, 362, 329	2.01×10^5	2.12×10^5	219, 142, 30
$[Ru(Py)_4PPIP]$	466, 359, 326	1.21×10^5	1.375×10^5	152, 79, 10
$[Ru(4\text{-}APy)_4(PIP)]$	461, 360, 307	7.5×10^4	7.23×10^4	208, 134, 20
$[Ru(Py)_4PIP]$	471, 361, 315	6.16×10^4	6.5×10^4	128, 81, 15

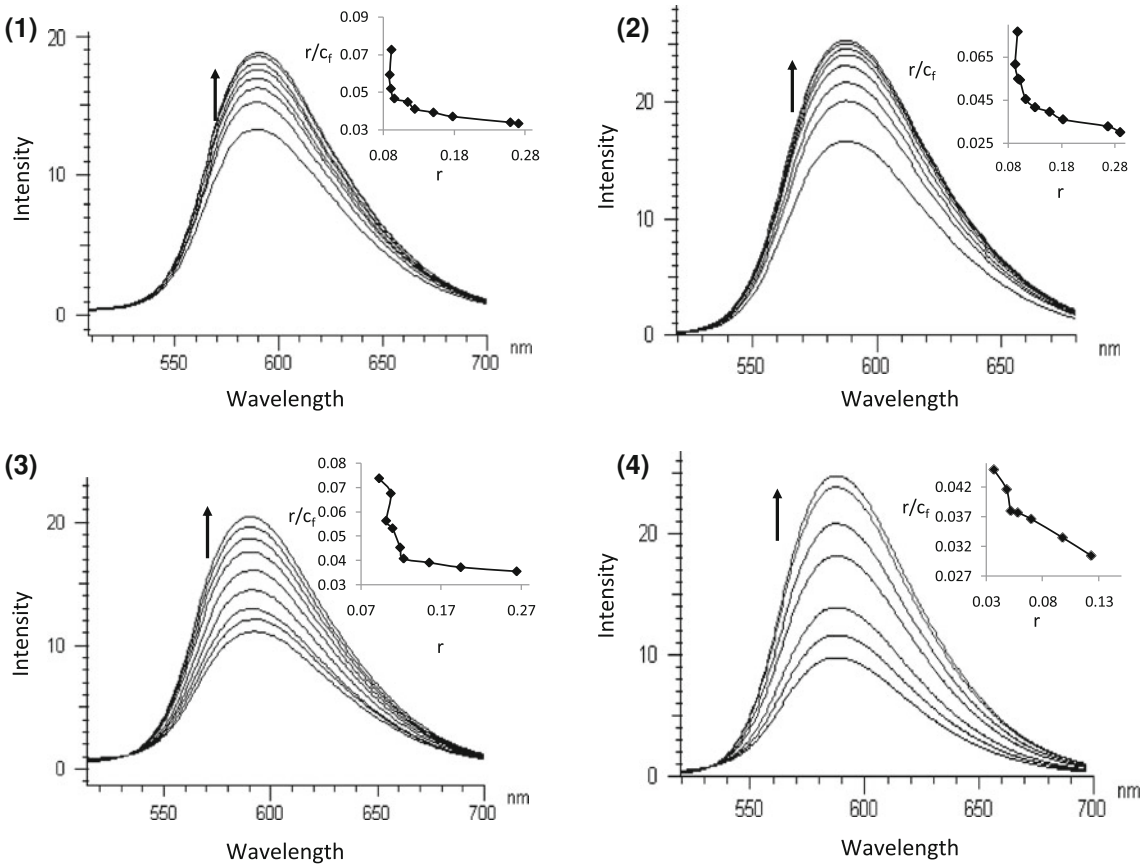

Fig. 3 Emission spectra of $[Ru(4\text{-}APy)_4(PPIP)](1)$, $[Ru(Py)_4PPIP](2)$ $[Ru(4\text{-}APy)_4(PIP)](3)$, $[Ru(Py)_4PIP](4)$ in Tris–HCl buffer at 25 °C upon addition of CT-DNA, [Ru] = 20 μM, [DNA] = 0–120 μM. The *arrow* shows the increase in intensity upon increasing CT-DNA concentrations

is an indication of the formation of non-luminescent species, Co^{2+}-$[Ru(APy)_4(PPIP)]$. The emission of DNA-intercalated complex (light switch on) can be quenched by transition metal ions, thus turning the light switch off, these are clearly demonstrated in Fig. 5. While adding EDTA into the (buffer) system containing Co^{2+}-$[Ru(APy)_4(PPIP)]$ or ($[Ru(APy)_4(PPIP)(Co)]^{4+}$), the emission intensity of the complex is recovered again (light switch on). This indicates that heterometallic complex Co^{2+}-$[Ru(APy)_4(PPIP)]$ becomes free again. In this experiment, adding 0.03 mM of Co^{2+} decreased the intensity of $[Ru(APy)_4(PPIP)]$ and on adding equimolar EDTA 0.03 mM the luminescence was recovered. Similar observations were obtained for all the four complexes.

Viscosity measurements

Though photo physical studies are quite useful in determining binding constants of metal complexes to DNA [36, 37], to further elucidate the binding mode of the present complexes, viscosity measurements were carried out. A classical intercalation model demands that the DNA helix lengthens as base pairs are separated to accommodate the binding ligand hence leads to an increase in the viscosity of DNA [38]. In contrast, a partial intercalation could bend the DNA helix and reduce its effective length and concomitantly its viscosity [39, 40]. The changes in relative viscosity of rod like CT-DNA in the presence of complexes

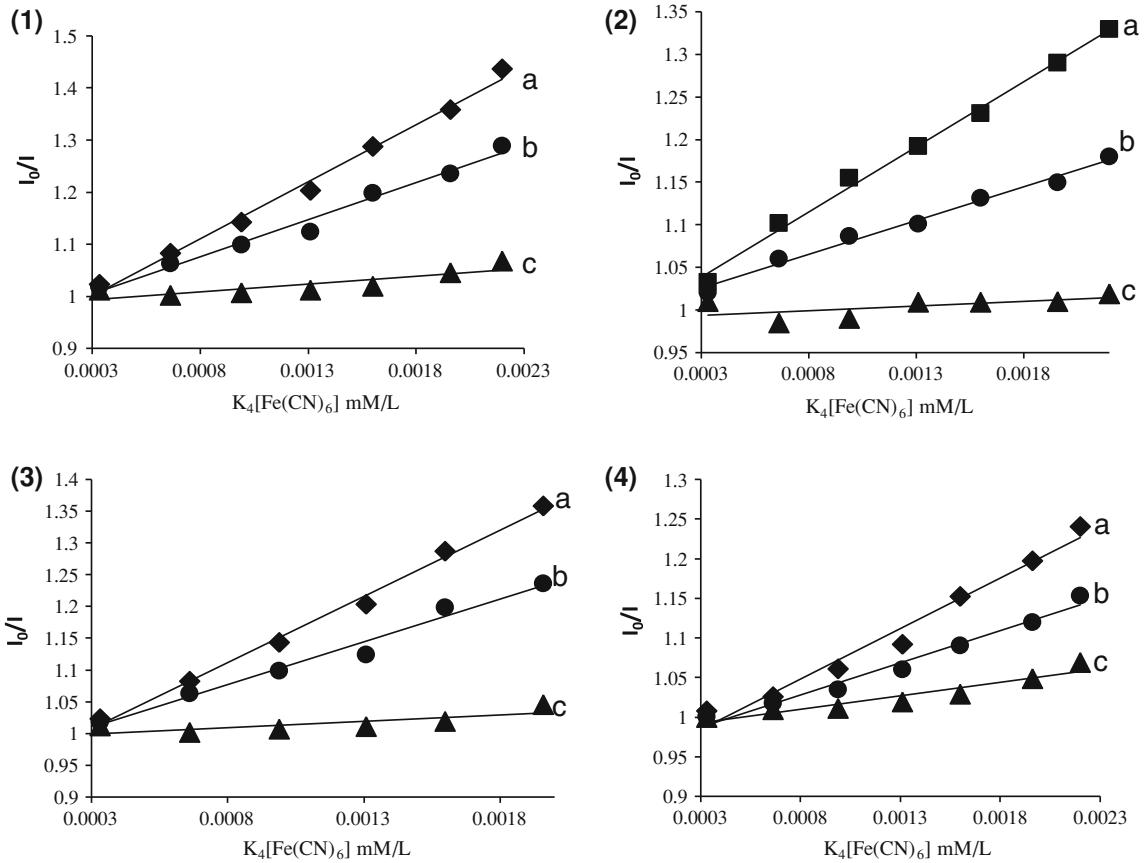

Fig. 4 Emission quenching of [Ru(4-APy)$_4$(PPIP)](1), [Ru(Py)$_4$PPIP] (2), [Ru(4-APy)$_4$(PIP)] (3) & [Ru(Py)$_4$PIP] (4) with $K_4[Fe(CN)_6]$ in the absence (**a**) and presence (**b**) [Ru] = 20 μm, and excess of DNA (**c**)

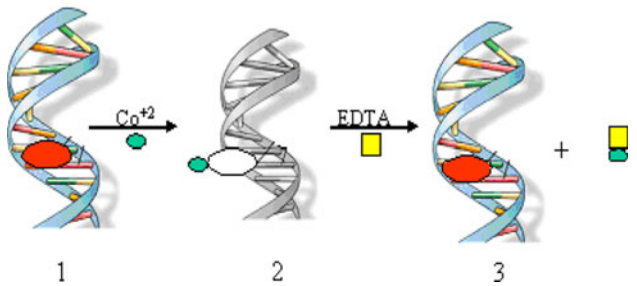

Fig. 5 Schematic representation of molecular light switch properties of [Ru(4-APy)$_4$(PPIP)] in presence of DNA (*1*) (switch on), in presence of Co(II) (switch off) (*2*) (heterometallic complex) and recovered luminescence upon addition of EDTA (*3*)

1, **2**, **3** and **4** are shown in Fig. 7. Ethidium bromide, a well-known DNA intercalator, increases the relative viscosity strongly by lengthening the DNA double helix through intercalation. As seen from Fig. 7 upon increase in the amounts of complexes **1** and **2**, the relative viscosity of the DNA increases steadily similar to the behavior of ethidium bromide, whereas in complexes **3** and **4** the increase in viscosity is comparatively less. The increased degree of viscosity, which may depend on the biding affinity to DNA, follows the order **EB** > **1** > **2** > **3** > **4** (Fig. 7). These results also suggest that all four complexes intercalate between the base pairs of DNA and parallel the result obtained by absorption, fluorescence and quenching measurements. Based on the binding data and the viscosity experiment, we conclude that these four complexes bind to DNA by intercalation. But they do not intercalate as strongly as proven intercalators [36].

Salt-dependent studies

Figure 8 shows the salt dependence of **1** and **3** complexes binding to DNA and comparative data for proven intercalators. The clear dependence of the binding constants for these complexes upon Na^+ binding to DNA may be analyzed by polyelectrolyte theory [41]. From Record theory, slope of the lines in Fig. 8 provide an estimate of $Z\psi$, where Z is the charge on the complex and ψ is the fraction of counter ions associated with each DNA phosphate ($\psi = 0.88$ for double-stranded B-form DNA). The data in Fig. 8 show that the slopes of the lines are greater than 1, being -1.31 and -1.236 for **1** and **3** complexes, respectively. These values are less than the theoretically expected

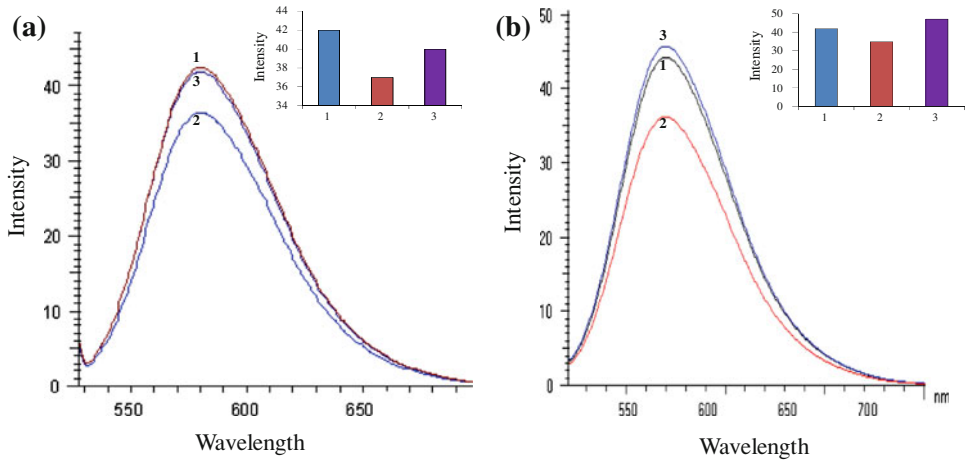

Fig. 6 Luminescence changes of 0.01 mM [Ru(PPIP)(APy)$_4$] in the presence of 0.2 mM of DNA (**a**), in the absence of 0.2 mM DNA (**b**) and (*1*), presence of 0.03 mM Co^{2+} (*2*) and addition of 0.03 mM of EDTA (*3*)

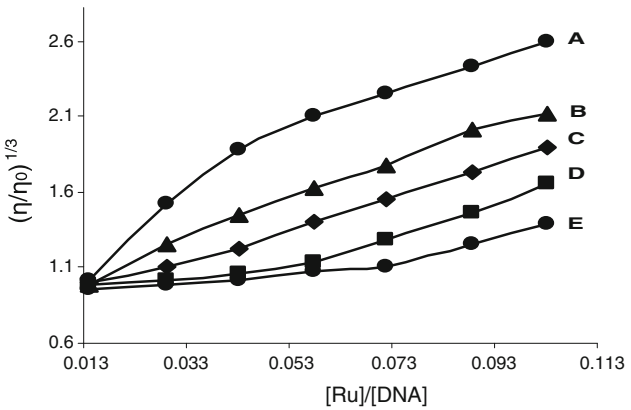

Fig. 7 Effect of increasing amount of ethidium bromide (**a**) [Ru(4-APy)$_4$(PPIP)] (**b**), [Ru(Py)$_4$PPIP] (**c**), [Ru(4-APy)$_4$(PIP)] (**d**) and [Ru(Py)$_4$PIP] (**e**) on relative viscosity of CT-DNA at 30 ± 0.1 °C. The total concentration of DNA is 0.25 mM

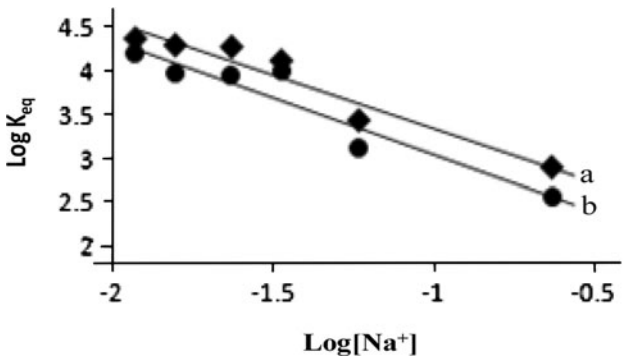

Fig. 8 Salt dependence of the equilibrium binding constants for DNA-binding ligands. Data are given for [Ru(4-APy)$_4$(PPIP)] (**a**) and [Ru(4-APy)$_4$(PIP)] (**b**). Slopes are −1.315 and −1.216, respectively

value of $Z\psi = 2 \times 0.88 = 1.76$. Such lower values could arise from coupled anion release (from the ligand) or from changes in ligand or DNA hydration upon binding. By increasing the Na^+ concentrations [42], the relative binding affinities of the complexes decreased similar to that of proven intercalators [43] like ethidium bromide.

Photocleavage of plasmid DNA by Ru(II) complexes

The potential of the present complexes to cleave DNA was studied by gel electrophoresis using supercoiled pBR 322 DNA. There has been considerable interest in DNA endonucleolytic cleavage reactions that are activated by metal ions. The delivery of high concentration of metal ion to the helix, in locally generating singlet oxygen ($^1O_2$) or hydroxyl radicals ·OH yields an efficient DNA cleavage reaction. Figure 9 shows gel electrophoresis separation of pBR 322 DNA after incubation with complexes and irradiation at 365 nm. No DNA cleavage was observed for control in which complex was absent (lane a). When this circular DNA was subjected to electrophoresis, relatively fast migration was observed for the supercoiled form (form I). As scission occurs on one strand, the supercoiled DNA generated electrophoretically slower-moving open circular form (form II). When both strands are cleaved, a linear form (III) was generated that migrated between forms I and II [44, 45]. With increasing concentrations of the complexes (lanes b–e), the amount of form I DNA diminished gradually, whereas form II increased. Further, the unirradiated control solution confirmed that the complexes did cause photosensitized cleavage. Under comparable experimental conditions, all complexes showed photocleavage activity.

Antimicrobial activity

Anticancer, antimicrobial activity and toxicological studies have been reported by our group [17, 18] for various Ru(II) complexes with polypyridyl ligands. Thus, antimicrobial activity was attempted for these complexes. The antibacterial activity was found in all four complexes. The antimicrobial activities of these compounds were determined

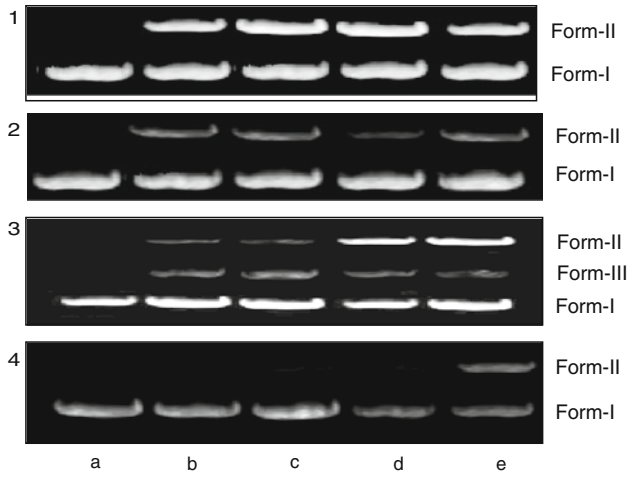

Fig. 9 Photo cleavage of pBR 322 DNA in the presence of [Ru(4-APy)$_4$(PPIP)] (*1*), [Ru(Py)$_4$PPIP] (*2*), [Ru(4-APy)$_4$(PIP)] (*3*) and [Ru(Py)$_4$PIP] (*4*) complexes, after irradiation with UV light at 365 nm. *Lane a* control plasmid DNA (untreated pBR 322), *lanes b–e* addition of complexes 20, 40, 60 and 80 μM

in vitro using different microorganisms by the standard disk method [46]. The antimicrobial activity data (Table 2) indicate that the complexes show appreciable activity against *E. coli* and *N. crassa*. The results were expressed as inhibition zone diameter (in mm). The complexes were more effective against *E. coli* than *N. crassa*. [Ru(Py)$_4$PIP] showed the highest activity (19 mm). When the same agar plates were supplemented with fungal species, it has been observed that the zone of inhibition was less. The antimicrobial activity increased as the concentration of the compounds increased. It is known that in a complex, the positive charge of the metal is partially shared with donor atoms present in the ligand and there may be π electron delocalization over the whole chelating ring. This increases the lipophilic character of the complex and favors its permeation through the lipid layer of the bacterial membrane [47, 48].

Conclusions

Four Ru(II) complexes containing monodentate auxiliary ligands have been synthesized and characterized. Binding of these complexes to CT-DNA has been investigated in detail by electronic absorption titration, steady state emission, viscosity and salt-dependent studies. The results suggest that all complexes bind to DNA in an intercalative mode. When irradiated at 365 nm, the four Ru(II) complexes were efficient photocleavers. Our studies lead us to conclude that as all four complexes are intercalators, they may be useful as a practical probe of DNA sequence or conformation. All the complexes show effects of light being switched on and switched off.

Table 2 Antibacterial activity of Ru(II) complexes at 20 μg/ml

	Bacterial species *E. coli*	Fungal species *N. crassa*
DMSO	Nil	Nil
[Ru(4-APy)$_4$(PPIP)]	12	9
[Ru(Py)$_4$PPIP]	10	8
[Ru(4-APy)$_4$(PIP)]	19	15
[Ru(Py)$_4$PIP]	6	1
Ampicillin	18–22	13–15

Values of zone of inhibition (mm, including the diameter of the disk)

Acknowledgments Council of Scientific and Industrial Research (CSIR), New Delhi, India. is greatfully acknowledged for the financial support in the form of Junior Research Fellow to C. Shobha Devi.

References

1. M.I. Romero, M. Rodriguez, A. Llobet, M.N. Cellomb-Dunand-Sauthier, A. Deronzier, T. Parella, H. Stoeckli-Evans, J. Chem. Soc. Dalton Trans. **11**, 1689–1694 (2000)
2. P. Belser, A. von Zelewsky, M. Frank, C. Seel, F. Vogtle, F. De Cola, V. Barigelletti, V. Balzani, J. Am. Chem. Soc. **115**, 4076–4086 (1993)
3. D.B. Hall, R.E. Holmlin, J.K. Barton, Nature **384**, 731–735 (1996)
4. C.J. Burrows, J.G. Muller, Chem. Rev. **98**, 1109–1151 (1998)
5. R.E. Holmlin, P.J. Dandliker, J.K. Barton, Angew. Chem. Ed. Eng. **36**, 2714 (1997)
6. M.J. Clarke, in *Metal Complexes in Cancer Chemotherapy*, ed. by B.K. Keppler (VCH, Weinheim, 1993), p. 129
7. B.K. Keppler, K.G. Lipponer, B. Stenzel, F. Kratz, in *Metal Complexes in Cancer Chemotherapy*, ed. by B.K. Keppler (VCH, Weinheim, 1993), p. 187
8. M.J. Clarke, F. Zhu, D.R. Frasca, Chem. Rev. **99**, 2511 (1999)
9. G. Sava, A. Bergamo, Int. J. Oncol. **17**, 353 (2000)
10. K.E. Erkkila, D.T. Odom, J.K. Barton, Chem. Rev. **99**, 2777 (1999)
11. L.-F. Tan, H. Chao, H. Li, Y.-J. Liu, B. Sun, W. Wei, L.-N. Ji, J. Inorg. Biochem. **99**, 513–520 (2005)
12. Y. Xiong, L.N. Ji, Coord. Chem. Rev. **185**, 711–733 (1999)
13. J.W. Mei, J. Liu, K.C. Zheng, L.J. Li, H. Chao Li, X. An, C.F. Yun, L.N. Ji, Dalton Trans. **27**, 1352–1359 (2003)
14. J.G. Liu, Q.L. Zhang, X.-F. Shi, L.N. Ji, Inorg. Chem. **40**, 5045–5050 (2001)
15. L.-M. Chen, J.-C. Chen, C.-P. Tan, C.-P. Tan, Shuo. Shi, K.-C. Zeng, L.-N. Ji, J. Inorg. Biochem. **102**, 330–341 (2008)
16. M. Mariappan, B.G. Maiya, Eur. J. Inorg. Chem. **11**, 2164–2174 (2005)
17. P. Nagababu, M. Shilpa, J.N. Latha, I. Bhatnagar, P.N.B.S. Srinivas, Y. Praveen kumar, S. Satyanarayana, J. Fluoresc. **21**, 563–572 (2011)
18. K. Ashwini kumar, K. Laxma reddy, S. Vidhisha, S. Satyanarayana, Appl. Organometal. Chem. **23**, 409–420 (2009)
19. J. Marmur, Mol. Biol. **3**, 208–218 (1961)
20. M.E. Reichmann, S.A. Rice, C.A. Thomas, P. Doty, J. Am. Chem. Soc. **76**, 3047–3053 (1954)

21. M. Yamada, Y. Tanaka, Y. Yoshimoto, S. Kuroda, I. Shimo Bull, Chem. Soc. Jpn **65**, 1006–1011 (1992)
22. L.-F. Tan, H. Chao, H. Li, Y.-J. Liu, B. Sun, W. Wei, L.-N. Ji, J. inog. Biochem. **99**, 513–520 (2005)
23. B.P. Sullivan, D.J. Salmon, T.J. Mayer, Inorg. Chem. **17**, 3334 (1978)
24. J.M. Kelly, A.B. Tossi, D.J. Mc Connell, C. Ohuigin, Nucleic-acids. Res. **13**, 6017–6034 (1985)
25. R.J. Morgan, S. Chatterjee, A.D. Baker, T.C. Strekas, Inorg. Chem. **30**, 2687 (1991)
26. S.A. Tysoe, R.J. Morgan, A.D. Baker, T.C. Stelkas, J. Phy. Chem. **97**, 1707–1717 (1993)
27. J.Z. Wu, L. Li, T.X. Zen, L.N. Ji, Polyhedron **16**, 103–107 (1997)
28. X.W. Liu, J. Li, K.C. Zheng, H. Chao, L.N. Ji, J. Inorg. Biochem. **99**, 2372–2380 (2005)
29. A.M. Pyle, J.P. Rehmann, R. Meshoyrer, C.V. Kumar, N.J. Turro, J.K. Barton, J. Am. Chem. Soc **111**, 3051–3058 (1989)
30. X.W. Liu, J. Li, H. Deng, K.C. Zheng, Z.W. Mao, L.N. Ji, Inorg. Chem. Acta. **358**, 3311 (2005)
31. R.B. Nair, E.S. Teng, S.L. Kirkland, C. Murphy, J. Inorg. Chem. **37**, 139–141 (1998)
32. J.B. Chairs, N. Dattagupta, D.M. Crothers, Biochemistry **24**, 3927–3932 (1982)
33. B.K. Ghosh, A. Chakravorty, Coord. Chem. Rev. **95**, 239 (1989)
34. X.-W. Liu, Y.-M. Shen, J.-L. Lu, Y.-D. Chen, L. Li, D.-S. Zhang, Spectrochemica Acta Part A Mol. Biomol. Spectrosc. **77**, 522–527 (2010)
35. M. Chen, H. Li, Q. Li, Z. Xu, Spectrochemica Acta Part A Mol. Biomol. Spectrosc. **75**, 1566–1570 (2010)
36. S. Satyanarayana, J.C. Dabrowiak, J.B. Chaires, Biochemistry **31**, 9319–9324 (1992)
37. G. Song, L. Ling, L. Liu, G. Fang, S. Lu, Z. He, Y. Zeng, Anal. Sci. **18**, 757–759 (2002)
38. C.V. Kumar, J.K. Barton, N.J. Turro, J. Am. Chem. Soc. **105**, 5518–5523 (1985)
39. J.K. Barton, A.T. Danishefsky, J. M. Goldberg, C.V. Kumar, N. J. Turro (1986)
40. J. Liu, W.J. Mei, L.J. Lin, K.C. Zhhen, H. Chao, F.C. Yun, L.N. Ji, Inorg.Chem. Acta **357**, 285 (2004)
41. M.T. Record, C.F. Anderson, T.M. Lohman, Q.Rev.Biophys. **11**, 103–178 (1978)
42. D.S. Sigma, A. Mazumder, D.M. Perrin, Chemical nucleases. Chem. Rev. **93**, 2295–2316 (1993)
43. S. Satyanarayana, J.C. Dabrowiak, J.B. Chaires, Biochemistry **32**, 2573–2584 (1993)
44. H. Johnston, C. Katherine, H. Glasgow, PH T. J. Am. Chem. Soc. **117**, 8933–8938 (1995)
45. M.H. Dalofo, B. Rodrigues, J.B. Kuhn, J. Brown, G. Wass, J.P. Maegroves, D.D. Von Hoff, E.K. Rowrty, Clin. Cancer Res. **4**, 2763–2770 (1998)
46. W.L. Drew, A.L. Barry, R.O. Toole, J.C. Sherris, Appl. Environ. Microbiol. **24**, 240 (1972)
47. Y. Anjaneyulu, R.P. Rao, Synth. React. Inorg. Met. Org. Chem. **16**, 257 (1986)
48. L. Mishra, V.K. Singh, Ind. J. Chem. **32**(A), 446 (1997)